

# ChemComm

Accepted Manuscript



This is an *Accepted Manuscript*, which has been through the Royal Society of Chemistry peer review process and has been accepted for publication.

*Accepted Manuscripts* are published online shortly after acceptance, before technical editing, formatting and proof reading. Using this free service, authors can make their results available to the community, in citable form, before we publish the edited article. We will replace this *Accepted Manuscript* with the edited and formatted *Advance Article* as soon as it is available.

You can find more information about *Accepted Manuscripts* in the [Information for Authors](#).

Please note that technical editing may introduce minor changes to the text and/or graphics, which may alter content. The journal's standard [Terms & Conditions](#) and the [Ethical guidelines](#) still apply. In no event shall the Royal Society of Chemistry be held responsible for any errors or omissions in this *Accepted Manuscript* or any consequences arising from the use of any information it contains.

## COMMUNICATION

# Water Proton NMR — A Sensitive Probe of Solute Association

Cite this: DOI: 10.1039/x0xx00000x

Yue Feng, Marc B. Taraban and Yihua Bruce Yu\*

Received 00th January 2012,

Accepted 00th January 2012

DOI: 10.1039/x0xx00000x

www.rsc.org/

**It is found that the transverse relaxation rate  $R_2$  of the water protons can be used to quantify protein aggregation and surfactant micellization in water. The simplicity and high intensity of the water proton signal enables non-invasive chemical analysis not readily achievable through solute proton signals, such as inspecting finished biologic products.**

The water proton signal played a critical role in the discovery of nuclear magnetic resonance (NMR).<sup>1</sup> But when monitoring chemical processes in aqueous solutions, contemporary NMR spectroscopy relies on signals from the solute (reactant or product) and typically regards the water proton signal as unwanted background to be eliminated through either solvent deuteration or signal suppression.<sup>2</sup> The underlying assumption is that the solvent proton signal is not informative of solute chemistry. While the solute NMR signals are indeed highly sensitive toward local changes such as bond formation, the water proton signal might be better at reporting global changes because the solute is immersed in water and thereby its global changes such as association are likely to affect many water molecules per solute molecule.

In a recent study, we found that the water proton transverse relaxation rate  $R_2$  can sense the stiffness of hydrogels while its longitudinal counterpart  $R_1$  displays no such sensitivity.<sup>3</sup> Decades ago, it was reported that the water proton  $R_2$  is more sensitive than  $R_1$  toward protein aggregation.<sup>4</sup> As gelation and aggregation both involve solute association, we decided to explore using the water proton  $R_2$  to monitor and possibly quantify solute association.

We first explored using the water proton signal to quantify protein aggregation, an issue of great concern to the biotechnology industry and regulatory agencies.<sup>5</sup> The protein proton signals are too weak and too complex for this purpose (Figure S1). In contrast, the water proton signal is much more intense and readily identifiable regardless of the complexity of the protein proton signals.

It is known that in the absence of aggregation, the water proton  $R_2$  increases linearly with protein concentration.<sup>6</sup> At a given protein concentration, aggregation will elevate the water proton  $R_2$ .<sup>4,7</sup> We confirmed these prior observations using bovine serum albumin (Figure S2). Missing from these previous studies is whether the magnitude of the water proton  $R_2$  correlates with the quantitative characteristics of protein aggregates, such as the average molecular weight  $\overline{M.W.}$ , the average hydrodynamic radius  $R_h$ , etc. Such correlations make it possible to quantify protein aggregation via the water proton  $R_2$ .

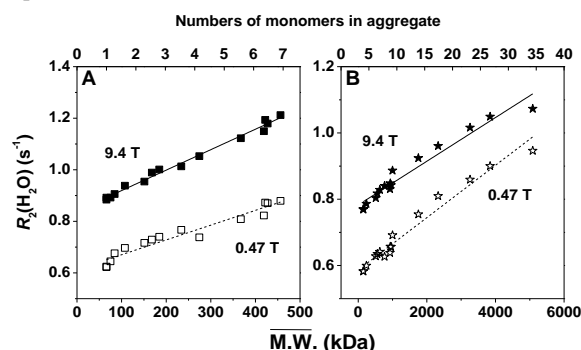
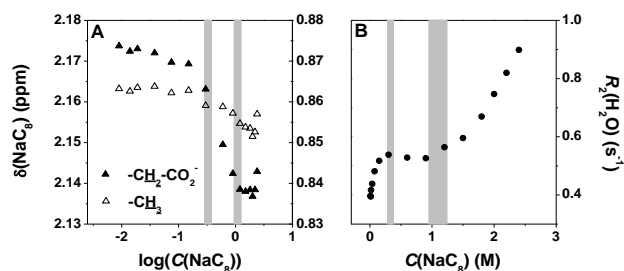


**Fig. 1** Quantifying protein aggregation via water proton NMR. (A). Increase of the water proton  $R_2$  with  $\overline{M.W.}$  of BSA aggregates at 9.4 T and 0.47 T. The goodness of linear fitting is 0.99 at 9.4 T and 0.94 at 0.47 T. (B). Increase of the water proton  $R_2$  with  $\overline{M.W.}$  of  $\gamma$ -globulin aggregates at 9.4 T and 0.47 T. The goodness of linear fitting is 0.95 at 9.4 T and 0.97 at 0.47 T. In both (A) and (B), the protein concentration was fixed at 15 mg/mL. The extent of aggregation was controlled by varying the heating temperature and duration.

Heat-induced aggregation of bovine serum albumin (BSA, 66 kDa) and  $\gamma$ -globulin (150 kDa) was conducted at constant protein concentration (15 mg/mL), pH 7.4 in phosphate-buffered saline (50 mM sodium phosphate, 100 mM sodium chloride). BSA and  $\gamma$ -globulin were selected because they represent the typical size of

protein therapeutics. The extent of aggregation was controlled by adjusting the temperature (55 °C or 60 °C) and duration (0 – 30 min) of heating.  $\overline{M.W.}$  and  $R_h$  of protein aggregates in each sample were calculated from the particle size distribution determined by dynamic light scattering (DLS).<sup>8</sup> As shown in Figures 1A& 1B, the water proton  $R_2$  increases with  $\overline{M.W.}$  of protein aggregates in an approximately linear fashion for both BSA and  $\gamma$ -globulin. Further, for each protein, this linear correlation between the water proton  $R_2$  and aggregate  $\overline{M.W.}$  holds equally well for  $R_2$  measured at both high (9.4 T, 400 MHz resonance frequency for  $^1\text{H}$ ) and low (0.47 T, 20 MHz resonance frequency for  $^1\text{H}$ ) magnetic field strength. Similar correlation between the water proton  $R_2$  and the average hydrodynamic radius  $R_h$  of protein aggregates is shown in Figure S3. These results demonstrate that the water proton signal is better suited than the protein proton signals to quantify protein aggregation. The advantage of the water proton signal comes from its simplicity and huge intensity (Figure S1).

Surfactant micellization presents another opportunity for water proton NMR. Unlike proteins, the surfactant proton signals are simple enough to be used to monitor micelle formation.<sup>9</sup> However, the surfactant proton signals might be insensitive toward subsequent micelle growth if such growth exerts little impact on surfactant hydrocarbons already buried deep inside the micelle core. One notable example of surfactants with a complex micellization process is sodium octanoate ( $\text{NaC}_8$ ), an anionic fatty acid surfactant.<sup>10</sup> Figure 2A plots two micellization profiles of  $\text{NaC}_8$  obtained respectively from the chemical shift of the  $\text{C}^2$  methylene protons and from that of the  $\text{C}^8$  methyl protons (see Figure S4 for the structure and  $^1\text{H}$  spectrum of  $\text{NaC}_8$ ). Both sets of data are noisy, consistent with published chemical shift data of the same two sets of protons in  $\text{KC}_8$  micellization.<sup>11</sup> The  $\text{C}^2$  methylene proton chemical shift profile displays two turning points matching respectively the reported 1<sup>st</sup> and 2<sup>nd</sup> critical micelle concentrations (CMCs) of  $\text{NaC}_8$ . The  $\text{C}^8$  methyl proton chemical shift profile displays only one hardly visible turning point near the reported 1<sup>st</sup> CMC of  $\text{NaC}_8$ . Further, the chemical shift of the  $\text{C}^8$  methyl protons changed to a much lesser extent than that of the  $\text{C}^2$  methylene protons in the micellization process. These results are consistent with the  $\text{C}^8$  methyl protons being buried much deeper inside the micelle core than the  $\text{C}^2$  methylene protons, and as such, they are much less sensitive toward micelle growth as compared to protons closer to the micelle surface. Of note, the chemical shift profile of neither set of surfactant hydrocarbon protons resembles the  $\text{NaC}_8$  micellization profiles established by other techniques such as partial specific volumes of water and  $\text{NaC}_8$ , xylene solubilization, and solution viscosity.<sup>10b, 12</sup>



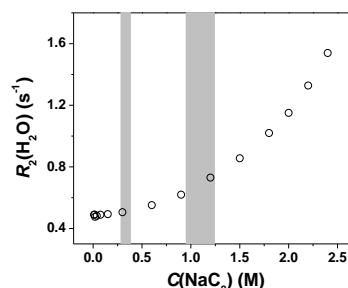
**Fig. 2** Monitoring  $\text{NaC}_8$  micellization via the surfactant (A) and water (B) proton signals at 9.4 T. In each panel, the two vertical grey bars indicate the reported 1<sup>st</sup> and 2<sup>nd</sup> CMC ranges of  $\text{NaC}_8$ , which are respectively 0.3 – 0.4 mol/kg (equivalent to 0.29 – 0.38 M) and 1.1 – 1.5 mol/kg (equivalent to 0.95 – 1.24 M).<sup>10b</sup> In (A), the left ordinate is the  $\text{C}^2$  methylene proton chemical shift and the right ordinate is the  $\text{C}^8$  methyl proton chemical shift. The  $\text{NaC}_8$  proton chemical shift data in (A) are plotted on the semi-logarithmic scale to facilitate comparison with published  $\text{KC}_8$  proton chemical shift data.<sup>11</sup>

Figure 2B plots the water proton  $R_2$  profile during  $\text{NaC}_8$  micellization. The water proton  $R_2$  data are much smoother than the surfactant hydrocarbon proton chemical shift data and clearly reveal two transitions with turning points matching respectively the reported 1<sup>st</sup> and 2<sup>nd</sup> CMCs of  $\text{NaC}_8$ .<sup>10b</sup> More importantly, the water proton  $R_2$  profile resembles the  $\text{NaC}_8$  micellization profiles established by other techniques.<sup>10b, 12</sup> The side-by-side comparison shown in Figure 2 demonstrates that the water proton signal is more sensitive toward  $\text{NaC}_8$  micellization than the surfactant proton signals. The higher sensitivity of the water proton signal is understandable because  $\text{NaC}_8$  micelle formation and growth involve the rearrangement and displacement of many water molecules at the micelle surface.<sup>13</sup>

The results on protein aggregation and surfactant micellization suggest that the water proton signal is indeed sensitive toward solute association in aqueous solutions. Hills and coworkers have shown previously that water-solute proton exchange underlies the sensitivity of the water proton  $R_2$  towards protein aggregation.<sup>7</sup> However, water-solute proton exchange cannot explain the sensitivity of the water proton  $R_2$  toward  $\text{NaC}_8$  micellization because  $\text{NaC}_8$  has no exchangeable protons. One might suggest that the diamagnetic susceptibility contrast between water and  $\text{NaC}_8$  underlies this sensitivity. The volume diamagnetic susceptibility,  $\chi_v$ , of water is  $-9.05 \times 10^{-6}$  while that of octanoic acid is  $-7.87 \times 10^{-6}$  (both in SI unit).<sup>14</sup> Upon micelle formation, this diamagnetic susceptibility contrast  $\Delta\chi_v$  between water and  $\text{NaC}_8$  will produce a local magnetic field gradient at the water-micelle interface. Local magnetic field gradient accelerates spin de-coherence and thus elevates the water proton  $R_2$ .<sup>15</sup> When spin diffusion is fast, as is the case of water,<sup>16</sup> the impact of the internal magnetic field gradient on spin de-coherence cannot be fully eliminated by the spin-echo technique.<sup>17</sup>

If the local magnetic field gradient at the water-micelle interface indeed underlies the observed water proton  $R_2$  sensitivity toward  $\text{NaC}_8$  micellization, then this sensitivity should diminish when the magnetic field strength of the NMR spectrometer is lowered or when the water-surfactant diamagnetic susceptibility contrast  $\Delta\chi_v$  is reduced. We put both predictions to test.

Figure 3 plots the water proton  $R_2$  profile obtained at 0.47 T during  $\text{NaC}_8$  micellization. In sharp contrast to the water proton  $R_2$  profile at 9.4 T (Figure 2B), the profile at 0.47 T displays no clear transition and no longer resembles the  $\text{NaC}_8$  micellization profiles established by other techniques.<sup>10b, 12</sup> Hence, a 20-fold reduction of the magnetic field strength of the NMR spectrometer from 9.4 to 0.47 T greatly diminished the sensitivity of the water proton  $R_2$  toward  $\text{NaC}_8$  micellization.



**Fig. 3** Monitoring  $\text{NaC}_8$  micellization via the water proton  $R_2$  at 0.47 T. The two vertical grey bars indicate the reported 1<sup>st</sup> and 2<sup>nd</sup> CMC ranges of  $\text{NaC}_8$ , which are respectively 0.3 – 0.4 mol/kg (equivalent to 0.29 – 0.38 M) and 1.1 – 1.5 mol/kg (equivalent to 0.95 – 1.24 M).<sup>10b</sup>

To explore the consequence of reduced  $\Delta\chi_v$  between water and the surfactant, micellization of sodium perfluorooctanoate ( $\text{NaFC}_8$ ) was investigated. Although the exact  $\Delta\chi_v$  value of  $\text{NaFC}_8$  is not known,

fluorinated molecules in general, but especially perfluorinated ones, have diamagnetic susceptibility much closer to water than their hydrogenated counterparts (see Table S1 for examples).<sup>18</sup> Hence  $\Delta\chi_v$  between water and NaFC<sub>8</sub> is expected to be much smaller than  $\Delta\chi_v$  between water and NaC<sub>8</sub>. Figure 4 plots the water proton  $R_2$  vs. NaFC<sub>8</sub> concentration  $C$  at 9.4 T and 0.47 T. At both magnetic field strengths, the water proton  $R_2$  data are quite noisy and no turning point near the reported CMC of NaFC<sub>8</sub> could be unambiguously identified. Hence reducing the diamagnetic susceptibility contrast  $\Delta\chi_v$  between water and the surfactant obscured the sensitivity of the water proton  $R_2$  toward micellization in this case.

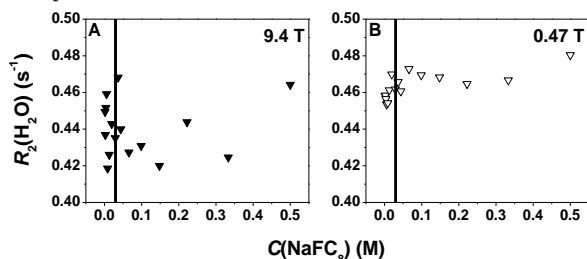


**Fig. 4** Water proton  $R_2$  vs. NaFC<sub>8</sub> concentration  $C$  at 9.4 T (A) and 0.47 T (B). The vertical line in each panel indicates the reported CMC of NaFC<sub>8</sub>, which is 0.03 M.<sup>19</sup>

Note that for NaC<sub>8</sub>, as the surfactant concentration increases from 0.09 M to 2.4 M, the water proton  $R_2$  grows larger at 0.47 T (by 1.0  $\text{s}^{-1}$ ) than at 9.4 T (by 0.5  $\text{s}^{-1}$ ). This is probably caused by the contamination of the water proton signal by the surfactant proton signals. The benchtop NMR spectrometer used in this study cannot separate water and surfactant proton signals and uses the CPMG echo amplitude to extract  $T_2$ . Such signal contamination becomes especially pronounced at high surfactant concentration, leading to larger growth of the apparent water proton  $R_2$ . This conclusion is supported by the results of NaFC<sub>8</sub>, where the water proton  $R_2$  varies to a lesser extent at 0.47 T than at 9.4 T (Figure 4). Because NaFC<sub>8</sub> contains no proton, the water proton  $R_2$  is not contaminated by surfactant proton relaxation.

The experimental results from NaC<sub>8</sub> and NaFC<sub>8</sub> at 9.4 T and 0.47 T indicate that the water-surfactant diamagnetic susceptibility contrast  $\Delta\chi_v$  underlies the sensitivity of the water proton  $R_2$  sensitive toward micellization. In the case of BSA and  $\gamma$ -globulin, the observed water proton  $R_2$  increase upon aggregation likely has contributions from both water-protein proton exchange and water-protein susceptibility contrast. This is because proteins have not only labile protons for exchange with water but also diamagnetic susceptibility contrast with water.<sup>20</sup> The fact that the water proton  $R_2$  is about equally sensitive at 9.4 T and 0.47 T toward protein aggregation suggests that water-protein proton exchange is probably the dominant contributor. Unlike local magnetic field gradient, water-solute proton-exchange is independent of the magnetic field strength of the NMR spectrometer.

In conclusion, this work demonstrates that water proton NMR provides a simple and effective alternative to solute proton NMR in monitoring solute association in aqueous solutions. In general, as the solute is surrounded by water, its chemical changes, especially large scale changes such as association, would inevitably impact its neighbouring water molecules. What unique of NMR is the long relaxation times of nuclear spins in water, which are on the order of seconds. In comparison, the relaxation times of water in infrared and Raman spectroscopy are on the order of picoseconds.<sup>21</sup> The long NMR relaxation times of water nuclear spins, along with rapid diffusion/exchange, make it possible for the impact of solute on water to propagate from the water-solute interface to bulk water.<sup>16</sup> In essence, water acts as an amplifier of solute chemistry. Both water-

solute proton exchange and water-solute diamagnetic susceptibility contrast contribute to this amplification process.

The simplicity and high intensity of the water proton signal enables non-invasive radiology-like chemical analysis that cannot be readily achieved with solute proton signals. One potential application is aggregation detection in biopharmaceutical products. Currently, aggregation in finished vials of protein therapeutics is inspected visually,<sup>22</sup> which brings significant subjectivity and variability and will miss the invisible aggregates (Figure S5). Visual inspection is used because all existing analytical methods are biopsy-like as they require taking the sample out of its original container and hence are not applicable to finished products inside sealed vials. In contrast, the water proton  $R_2$  can be readily measured using a benchtop NMR spectrometer without opening the vial (Figure S6).

The ability to quantify aggregation inside finished products fills an important gap in biologics quality control, which is how to verify the aggregation status of a protein drug at the point-of-care. This problem arises because improper transportation and storage conditions can cause aggregation and thereby harm the patient.<sup>23</sup> The inability to conduct post-manufacturing aggregation assessment constitutes a void in the regulation of biologics. The rapid growth of both innovator and follow-on biologics is likely to push the demand for a simple and affordable analytical technique capable of quantifying protein aggregation in finished products (vials, pre-filled syringes, etc.) at the point-of-care by end-users (pharmacists, nurses and even patients). Water proton  $R_2$  measurement using a benchtop or handheld NMR spectrometer offers one such possibility.

## Conclusions

This work demonstrates that water proton NMR provides a simple and effective method in monitoring solute association in aqueous solutions. This technique has many potential applications such as rapid and non-invasive quantification of protein aggregation in biopharmaceutical products.

## Notes and references

Department of Pharmaceutical Sciences, University of Maryland, Baltimore, MD, 21201, USA. E-mail: [byu@rx.umaryland.edu](mailto:byu@rx.umaryland.edu)

This work was supported by sequentially the NSF (CBET 1133908), the FDA (through M-CERSI) and the Maryland Technology Development Corporation (through MII). The DLS experiments were conducted at the Light Scattering Center of the University of Maryland College Park.

†Electronic Supplementary Information (ESI) available: [Experimental procedures and characterization data]. See DOI: 10.1039/c000000x/

- 1 F. Bloch, W. W. Hansen and M. Packard, *Phys. Rev.*, 1946, **69**, 127.
- 2 G. Zheng and W. S. Price, *Prog. Nucl. Magn. Reson. Spectrosc.*, 2010, **56**, 267.
- 3 Y. Feng, M. B. Taraban and Y. B. Yu, *Chem. Commun.*, 2014, **50**, 12120.
- 4 J. Oakes, *J. Chem. Soc. Faraday Trans. 1*, 1976, **72**, 228.
- 5 (a) *Aggregation of Protein Therapeutics*, ed. W. Wang and C. J. Roberts, Wiley, Hoboken, NJ, 2010; (b) A. S. Rosenberg, D. A. Verthelyi, and B. W. Cherney, *J. Pharm. Sci.*, 2012, **101**, 3560.
- 6 (a) O. K. Daszkiewicz, J. W. Hennel, B. Lubas and T. W. Szczepkowski, *Nature* 1963, **200**, 1006; (b) J. Oakes, *J. Chem. Soc. Faraday Trans. 1* 1976, **72**, 216; (c) B. P. Hills, S. F. Takacs and P. S. Belton, *Mol. Phys.*, 1989, **67**, 903.
- 7 B. P. Hills, S. F. Takacs and P. S. Belton, *Mol. Phys.*, 1989, **67**, 919.
- 8 T. Arakawa, J. S. Philo, D. Ejima, K. Tsumoto and F. Arisaka, *BioProcess Int.*, 2007, **5**, 36.
- 9 X. Cui, S. Mao, M. Liu, H. Yuan and Y. Du, *Langmuir* 2008, **24**, 10771.
- 10 (a) J. B. Rosenholm, *Adv. Colloid Interface Sci.*, 1992, **41**, 197; (b) P. Ekwall, *Chemistry, Physics and Application of Surface Active*

- Substances*, Vol. 2, ed. J. Th. G. Overbeek, Gordon and Breach, New York, 1967, pp. 651-658.
- 11 M. A. Desando and L. W. Reeves, *Can. J. Chem.*, 1986, **64**, 1823.
  - 12 P. Ekwall, H. Eikrem and L. Mandell, *Acta Chem. Scand.*, 1963, **17**, 111.
  - 13 P. Ekwall and P. Holmberg, *Acta Chem. Scand.*, 1965, **19**, 573.
  - 14 *CRC Handbook of Chemistry and Physics*, ed. D. R. Lide, CRC Press, Boca Raton, 84th edn., 2003-2004.
  - 15 J. F. Schenck, *Med. Phys.*, 1996, **23**, 815.
  - 16 J. A. Glazer and K. H. Lee, *J. Am. Chem. Soc.*, 1974, **96**, 970.
  - 17 (a) R. J. S. Brown and P. Fantazzini, *Phys. Rev. B*, 1993, **47**, 14823; (b) S. Michaeli, et al. *Magn. Reson. Med.*, 2002, **47**, 629; (c) O. Speck, M. Weigel and K. Scheffler, *High-field MR Imaging*, ed. J. Hennig, and O. Speck, Springer, Berlin, 2011, pp. 89.
  - 18 M. P. Krafft, *Adv. Drug Delivery Rev.*, 2001, **47**, 209.
  - 19 N. Muller and H. Simsohn, *J. Phys. Chem.*, 1971, **75**, 942.
  - 20 (a) J. P. Savicki, G. Lang and M. Ikeda-saito, *Proc. Natl. Acad. Sci. USA* 1984, **81**, 5417; (b) J. S. Philo, U. Dreyer and T. M. Schuster, *Biochemistry* 1984, **23**, 865; (c) J. Luo, et al. *J. Magn. Reson.*, 2010, **202**, 102.
  - 21 (a) H. K. Nienhuys, S. Woutersen, R. A. van Santen and H. J. Bakker, *J. Chem. Phys.*, 1999, **111**, 1494; (b) K. Mizoguchi and Y. Tominaga, *J. Chem. Phys.*, 1992, **97**, 1961.
  - 22 L. D. Torbeck, *Pharm. Tech.*, 2010, **34**, 34.
  - 23 (a) F. Fotiou, S. Aravind, P. P. Wang and O. Nerapusee, *Clin. Ther.*, 2009, **31**, 336; (b) F. Locatelli, L. D. Vecchio and P. Pozzoni, *Peri. Dialys. Int.*, 2007, **27**, S303.